Int J Adv Manuf Technol (2013) 68:149–164
DOI 10.1007/s00170-012-4715-x

ORIGINAL ARTICLE

Propagation of assembly errors in multitasking machines by the homogenous matrix method

E. Díaz-Tena · U. Ugalde · L. N. López de Lacalle · A. de la Iglesia · A. Calleja · F. J. Campa

Received: 13 February 2012 / Accepted: 26 December 2012 / Published online: 22 January 2013

Abstract In this work, a methodology for the assessment of the geometrical accuracy of a multiaxis machine, the type usually called multitasking machine, was fully developed. For this purpose, the well-known formulation by Denavit and Hartenberg was applied. Multitasking machines are derived from lathes in which turrets are substituted by milling spindles, or they are also derived from milling centres including a turning headstock on the machine bed. In both cases, they are kinematically much more complex than lathes or milling centres, where it is not easy to previously calculate the consequence of parallelism and squareness errors between elements and joints. In this paper, a radical new 'multitasking' machine model was studied. Literature shows a complete lack of values for this kind of machine. In the methodology presented here, errors were introduced as additional geometric parameters in each elemental transformation matrices, resulting in the real transformation matrix for a multitasking machine. Elemental errors and the way to introduce them into the Denavit and Hartenberg matrices are fully described. Some simulations are tested, giving a useful outcome regarding the sensitivity of the machine with respect to the feasible assembly errors or errors produced by light misalignments caused by the machine tool continuous use.

Keywords Multi-axis machining centres · Accuracy · Precision · Geometrical errors

E. Díaz-Tena · U. Ugalde · L. N. López de Lacalle (✉) · A. de la Iglesia · A. Calleja · F. J. Campa
Department of Mechanical Engineering, University of the Basque Country, ETSI, C/Alameda de Urquijo s/n, 48013 Bilbao, Spain
e-mail: implomal@bi.ehu.es

1 Introduction

To date, multitasking machines are increasing in use in a lot of workshops since their appearance on industrial exhibition fairs in the middle 1990s. In the last 15 years, new models with radical new machine structure have been designed, assembled and purchased by workshops, asking for a new production point of view due to their superior capacities in productivity and accuracy terms. Multitasking machines' main structures can be divided into two main groups [1]:

- Structure of a lathe adding three aspects: the C control, a *Y*-axis perpendicular to the *X*–*Z* plane, and living tools in a turret or a milling spindle that is able to block its angular position.
- Structure of a four-axis milling machine (three linear and one rotary) where the bench is substituted by a turning headstock with additional control of the *C*-axis.

The development of this kind of machine is impossible to be referred without naming the trademarks and machine models. Since 1982, when WFL© launched the WNC 500S Millturn, lot of companies have been working to create new multitasking machines or to improve both structural and functional parts. Thenceforth, the evolution of these machines has been a continuous process. The most important advances could be: the launching of the Super Multitasking Machine 'STW-40' (Nakamura Tome©, 2000), the development of the NT series (Mori Seiki©, 2004) and the creation of the revolutionary concept of vertical lathe+milling centre based on customer requirements, conducted by GMTK© in the 2007s.

Currently, milling is a high added value production process where accuracy, short lead time and economical aspects must be simultaneously considered. Precision needs demanded by users are gradually increasing, including both

dimensional and geometrical requirements. Special activities are needed to obtain closed tolerances for precise machined components in minimum time (least rework). CNC machine tools are inevitable parts of precision production processes. Accurate machining by CNC machine tools is affected by a number of error sources based on specific parameters, including force and stress, geometrical deviations of machine structure and thermal variations.

Since the late 1990s, multiaxis milling centres have been widely used for the production of several-side parts in only one setup, or to produce complex surfaces by simultaneous interpolation of their 5 degrees of freedom, and in the 2000s, the multiaxis and multitasking machines irrupted. However, different errors inherent to the complexity of these machines increase the error on the quality of the final parts. The main error sources in machine tools [2, 3] are categorised as follows:

- *Geometric errors* [3–26], due to mechanical imperfections, such as axes misalignments, slideways and joints wear. These errors directly affect the relative position between tool and workpiece [4], producing dimensional errors. In three-axis machining centres error propagation is basically linear but not in machines with rotary axes.
- *Kinematics errors*, which are consequence of the machine lack ability to reach the exact position specified by the controller. Uncertainty in position of machine slides, gears backlash, couplers, motors, etc., is included in this error group [6].
- *Thermal errors* [2, 6, 26]—the main causes of thermal distortions are the global variation of the workshop temperature or local heating due to feed motors, chip heaps or main spindle heating.
- *Stiffness error* [27, 28]—machine tool is not perfectly rigid, so the weight of structural components causes large errors, highly dependent on the machine tool position.
- *Errors related with bending deformation of cutting tools and/or machine* [29–33]—there are important errors addressed to the deflection of cutting tools or distortion of the entire machine. Errors derived from tool deflection in ball-end finishing processes can exceed 40 μm or even more [32].

Error budget is a usual method for calculating the global uncertainty of a machine tool, as proposed by Donaldson [34], Slocum [4], Walter et al. [35] and Treib and Matthias [36]. The error budget procedure detects the sources of errors to be quantified, so that subsequent design and research efforts could be directed at those problems with mainly effect precision and accuracy. The budget must include all the elements that affect the final accuracy of the workpiece, i.e. the machine, the process, auxiliary equipment and the interactions between them [36]. Here and in Ref. [30], errors coming from the final assemble of machine structures were the first ones to be analysed.

Many researchers investigated geometric errors for three-axis machine tools from several points of view. Nawara et al. [7], Soons et al. [8] and Suh et al. [9] formulated the error of machine tools from 21 simple error components, and proposed a prediction and compensation algorithm for the geometric errors. Ferreira and Liu [10] investigated a modelling method for compensating errors in three-axis machine tools. Mou and Liu [11] developed a quadratic error model based on rigid-body kinematics. Cho et al. [13] presented a volumetric error model and applied it for precision machining of free-form surfaces. Fan et al. [26] investigated the effect of temperature on machine tools error and proposed methods for their measurement and compensation. Lee et al. [37] developed a general volumetric error model to synthesise all geometric error components of a three-axis miniaturised machine tool and proposed a recursive compensation method.

Nowadays, no reference about errors in multitasking machine has been found, but there were a few regarding five-axis milling centres [38]. Machining accuracy of five-axis machines is generally inferior to conventional ones, because those with two rotary axes can suffer numerous deviations in the assembly procedure of their mechanisms [5, 13–15]. On the other hand, the usual work of this kind of machine allows the production of very complex parts impossible to be manufactured in a three-axis machine. There are some measurement methods for identifying the geometric deviations of multi-axis machines, most of them using the Ball-bar method. Thus, in Lei et al. [15] the error values of a five-axis machine are calculated along the movements in X, Y, and Z, reaching volumetric errors diagrams for a real machine. Tsutsumi and Akinori [5] used the ball-bar methods for five-axis centres, and recently Zargasbashi and Mayer [39] study the trunnion-type A-axis. Ball-bar can also be used to estimate the geometric errors of a rotary table, as Lee et al. did [40]. The accuracy of five-axis milling machines has been studied by means of Denavit and Hartenberg formulation by Suh and Lee [9], by Mahbubur et al. [19] and by López de Lacalle et al. in Ref. [41], in the latter two in a similar way to the present work. Jha and Kumar [14] studied the influence of straightness errors on the profiling of a CAM but did not take into account other geometric deviations, as it is done in the present work, where straightness is not considered so it is the complementary view. Other possibility to Denavit and Hartenberg is the use of the mechanisms screw theory, used by Sang-Ku Moon et al. [21].

International standards [42–44] include tests and admissible tolerances for checking linear axes and some tests to check rotary axes, mainly for bi-rotary heads in machines

with horizontal or vertical Z-axis. However, there are no tests to check five-axis or multiaxis machines with tilting tables. The second group includes procedures for positioning and interpolation control studying, based on laser interferometers, Ball-bar or static measurements using position sensors. The last group includes test parts to check the behaviour of milling centres during the machining process, but to date these tests are focused on three-axis milling centres only. The most known is the NAS workpiece (ISO 10791-7:1998 'Test conditions for machining centres —part 7: accuracy of a finished test piece') and the NC-Gesellschaft testpart [32]. However, none of them is included in the ISO standard normative.

With all this, and as there is an upward forecast in the use of multitasking machines, it is doubtless that a priori evaluation of the errors would be useful for a better design, construction, assembly and maintenance of multitasking machines. Furthermore, knowing the kind and the value of the errors during the manufacturing process, it gives the opportunity to compensate them, obtaining the final quality desired in the workpiece at a reduced cost.

The aim of this work is to study how an error in the structure of a multitasking machine could be propagated causing lack of precision in the workpiece. For that purpose, firstly Denavit and Hartenberg method is explained and secondly a multitasking machine is simplified to its kinematic configuration. In Section 3, comparing the theoretical and the real position, the consequences of introducing a squareness error, a clamping error and a misalignment error are calculated. Finally, how these errors change with machine position and the error effect in continuous machining is analysed.

2 Theoretical global transformation matrices in the machine under study

2.1 Homogeneous matrix method

Denavit and Hartenberg notation (proposed in 1955) relates the consecutive position of local reference systems associated to each element of a spatial manipulator, in our case a five-axis machine tool, to find the position of the tool grasped by the spatial manipulator. Other possibilities to calculate the final position of tool being used in three-axis are difficult to be applied in five-axis [23, 24].

The complex multi-axis machine structure is represented by a 'bar and nodes' kinematics scheme. Thus, by means of the product of the transformations between successive coordinate systems associated to the mechanisms elements, from the absolute (X_1 Y_1 Z_1) reference system to the 'tool centre point' system (X_{tcp} Y_{tcp} Z_{tcp}), the *global transformation matrix* $\mathbf{T_{4\times4}}$ is obtained. This matrix is function of the geometrical parameters of structure and the position of the degrees of freedom (machine axes), and gives the final position of the tool. Each kinematics and each machine presents its own transformation matrix $\mathbf{T_{4\times4}}$.

In Denavit and Hartenberg method, the elements that take part on the machine structure are listed from the fixed element to the last element. Each element is connected to another one by means of kinematic joints, such as rotary and prismatic ones, having rotational axes or sliding axes respectively. A $X_iY_iZ_i$ reference system is given to each i element, being the origin of the coordinate system located on the joint with the element $i+1$ (see Fig. 1). To completely define the kinematic configuration of each element, the next parameters are required:

- *Element length* a_i, distance between Z_{i-1}- and Z_i-axes measured along the X_i axis.
- Element torsion α_i, angle between Z_{i-1}- and Z_i-axes, from Z_{i-1}-to Z_i in counterclockwise and from the positive direction of X_i.
- Distance between elements d_i, distance between X_{i-1} and X_i axes measured along the Z_{i-1}-axis.
- Joint angle θ_i, angle between X_{i-1}- and X_i-axes, from X_{i-1} to X_i in counterclockwise and from the positive direction of Z_{i-1}.

Element length and element torsion define the element itself, while the other parameters define the relative position between two adjacent elements.

The conversion from the $i-1$ system to the i system is performed through four simple transformations:

1. A rotation θ_i about the Z_{i-1} axis to bring X_{i-1} parallel with X_i.

$$\mathbf{T}_{\theta_i,Z_{i-1}} = \begin{bmatrix} \cos\theta_i & -\sin\theta_i & 0 & 0 \\ \sin\theta_i & \cos\theta_i & 0 & 0 \\ 0 & 0 & 1 & 0 \\ 0 & 0 & 0 & 1 \end{bmatrix} \quad (1)$$

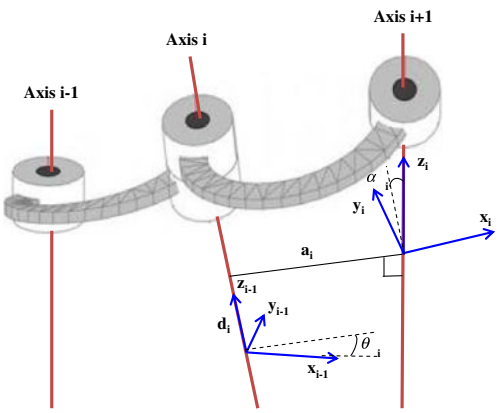

Fig. 1 Denavit and Hartenberg parameters [45]

2. A translation d_i along the Z_{i-1} axis to make the X-axes collinear.

$$\mathbf{T}_{d_i,Z_{i-1}} = \begin{bmatrix} 1 & 0 & 0 & 0 \\ 0 & 1 & 0 & 0 \\ 0 & 0 & 1 & d_i \\ 0 & 0 & 0 & 1 \end{bmatrix} \tag{2}$$

3. A translation a_i along the X_i-axis to make the Z-axes coincide.

$$\mathbf{T}_{a_i,X_i} = \begin{bmatrix} 1 & 0 & 0 & a_i \\ 0 & 1 & 0 & 0 \\ 0 & 0 & 1 & 0 \\ 0 & 0 & 0 & 1 \end{bmatrix} \tag{3}$$

4. And, a rotation α_i about the X_i-axis to bring Z_i parallel and coincident with Z_{i+1}.

$$\mathbf{T}_{\alpha_i,X_i} = \begin{bmatrix} 1 & 0 & 0 & 0 \\ 0 & \cos\alpha_i & -\sin\alpha_i & 0 \\ 0 & \sin\alpha_i & \cos\alpha_i & 0 \\ 0 & 0 & 0 & 1 \end{bmatrix} \tag{4}$$

From these simple transformations, the *elemental transformation matrix* ${}^{i-1}_{i}\mathbf{T}$ is obtained:

$$\begin{aligned} {}^{i-1}_{i}\mathbf{T} &= \mathbf{T}_{\theta_i,Z_{i-1}} \cdot \mathbf{T}_{d_i,Z_{i-1}} \cdot \mathbf{T}_{a_i,X_i} \cdot \mathbf{T}_{\alpha_i,X_i} \\ &= \begin{bmatrix} \cos\theta_i & -\sin\theta_i\cos\alpha_i & \sin\theta_i\sin\alpha_i & a_i\cos\theta_i \\ \sin\theta_i & \cos\theta_i\cos\alpha_i & \cos\theta_i\sin\alpha_i & a_i\sin\theta_i \\ 0 & \sin\alpha_i & \cos\alpha_i & d_i \\ 0 & 0 & 0 & 1 \end{bmatrix} \end{aligned} \tag{5}$$

The multiplication of the elemental transformation matrices results in the *global transformation matrix of the system* $\mathbf{T_{4\times4}}$, in this case it is going to be noted as the *theoretical* $\mathbf{T_{th}}$ because it does not include the geometric errors:

$${}^{1}_{n}\mathbf{T}_{th} = \mathbf{T}_{12} \cdot \mathbf{T}_{23} \cdot \ldots \cdot \mathbf{T}_{n-1\,n} = \begin{bmatrix} u_x & v_x & w_x & \delta_x \\ u_y & v_y & w_y & \delta_y \\ u_z & v_z & w_z & \delta_z \\ 0 & 0 & 0 & 1 \end{bmatrix} \tag{6}$$

Dividing this matrix in the habitual sub-matrixes it results:

$${}^{1}_{n}\mathrm{T}_{th} = \begin{bmatrix} {}^{1}_{n}\mathbf{R}_{th} & {}^{1}_{n}\mathbf{d}_{th} \\ \mathbf{0} & 1 \end{bmatrix} \tag{7}$$

Where:

$${}^{1}_{n}\mathbf{R}_{th} = \begin{bmatrix} u_x & v_x & w_x \\ u_y & v_y & w_y \\ u_z & v_z & w_z \end{bmatrix} \tag{8}$$

Represents the orientation of the tool centre point respect of the original (X_1 Y_1 Z_1) coordinate system in the theoretical case, and

$${}^{1}_{n}\mathbf{d}_{th}{}^{T} = [\,d_x \quad d_y \quad d_z\,] \tag{9}$$

Represents the theoretical tool tip centre point position respect of the same system.

The multiplication between the global transformation matrix and the vector of the homogeneous coordinates referenced to the mobile coordinate system (tcp system) result is the coordinates of that vector related to the absolute coordinate system. In milling, the final element caught by the spatial manipulator is a cylinder, which represents the end mill tool. If the tcp is placed at the tool tip, its position in the absolute reference results from the transformation of the origin of the *tcp* coordinate system using its homogeneous coordinates (0,0,0,1).

$$\mathbf{X} = \mathbf{T}_{th} \cdot \mathbf{X}_{loc} \tag{10}$$

2.2 Structure and theoretical matrices for the multitasking machine under study

In Fig. 2, the multitasking machine model studied in this work is shown. As it can be seen, it is a multiaxis machine in which the three main Cartesian axes are solved by a box-in-box structure typical of horizontal milling centres, with a swivel rotation degree of freedom ram. On the bed is placed a horizontal headstock with the chuck plate and a counter chuck place on a sliding additional linear axis. Behind both plates is the turret with capacity for living tools and built-in motors. At the view of the picture, the absolutely and radical new design adding usual structures for milling centres and lathes in the same machine bed is easily deduced.

For the present work, the machine was simplified to a kinematical draft showing the degrees of freedom (axes), and including the usual elements used on theory of mechanism as it can be seen in Fig. 3.

The axis nomenclature used in Figs. 2 and 3 does not follow the ISO standard exactly. This is due to the presence

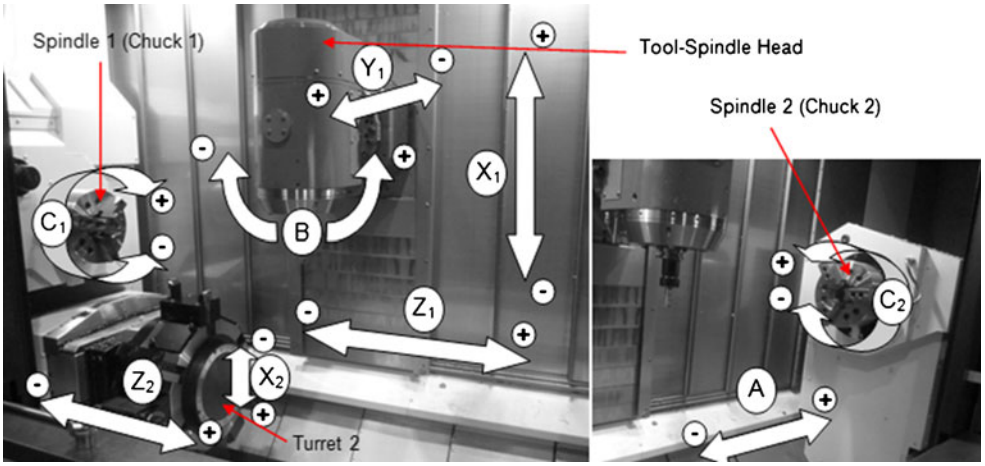

Fig. 2 The multitasking machine studied in this work and machine degrees of freedom also so-called axes

of several machine axes on the same direction along with several main spindles (headstock and counter-headstock spindles for turning and one for milling mount in the horizontal ram). Even the CN equipment interpolates each set of axes separately, usually so-calling each of the sets as 'channels'. However, the power of current numerical controls allows them working simultaneously in a collaborative way. Thus, in ISO 841: 2001 'Industrial automation systems and integration—numerical control of machines—coordinate system and motion nomenclature' there are parallel axes, but in machines with only one main spindle, therefore different to multitasking machines in which there are two or three spindles, as the case of Fig. 2. As it has been said, this case includes two lathe spindles, one high speed milling spindles mounted at the end of the octagonal ram, and a turning turret located under the lathe axis in which a built-in motor for living tools is also possible.

If the machine is considered ideal, without any structural defect, and Denavit and Hartenberg method is applied to the diagram, the coordinate systems shown in Fig. 4 is obtained. Here, axes remarked with circles correspond with those named by the machine manufacturer, whereas the italic marked ones are those derived from the systematic application of the Denavit and Hartenberg approach. In this figure two cylindrical parts are drown on both lathe main spindle (spindle 2) and counterspindle (spindle 1) only for illustrative purpose. The first and original reference point (of X_1, Y_1 and Z_1) is located in the workpiece reference, reaching the tool tip after several local transformations.

Once those axes are defined, all the transformation matrixes have to be developed. Firstly, the basic parameters required for the formation of the matrixes have to be calculated, as gathered in Table 1.

With these all, Denavit and Hartenberg general transformation matrix is applied to each element. Multiplying all of them the general transformation matrix is obtained. The transformation changes the movement from the C_1-axis (reference system X_1, Y_1 and Z_1) to the point of the tool (reference system X_{tcp}, Y_{tcp} and Z_{tcp}). All the matrixes can be found in Table 1.

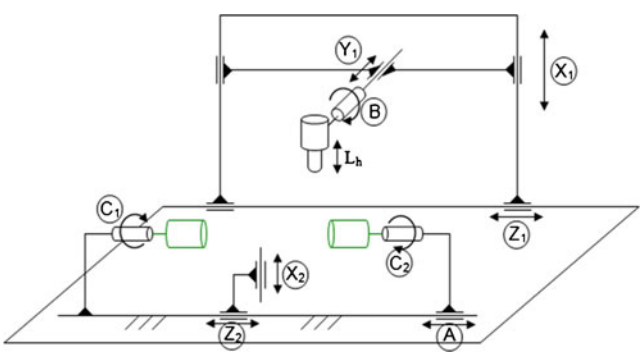

Fig. 3 Kinematic configuration of the machine

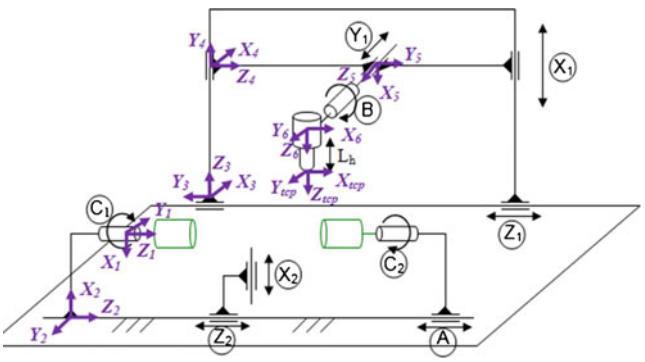

Fig. 4 General coordinate systems, for the 'channel' or set of axes 1

Table 1 Geometrical parameters of the Denavit and Hartenberg model, Channel 1

Transaction from element i-1 to element i	a_i	a_i	d_i	θ_i	*Transformation matrix*
12	*1400*	*0*	*-1140*	C_1+180	$T_{12}=\begin{bmatrix} -\cos(C_1) & \sin(C_1) & 0 & -1400\cos(C_1) \\ -\sin(C_1) & -\cos(C_1) & 0 & -1400\sin(C_1) \\ 0 & 0 & 1 & -1140 \\ 0 & 0 & 0 & 1 \end{bmatrix}$
23	*700*	*270*	Z_1	*270*	$T_{23}=\begin{bmatrix} 0 & 0 & 1 & 0 \\ -1 & 0 & 0 & -700 \\ 0 & -1 & 0 & Z_1 \\ 0 & 0 & 0 & 1 \end{bmatrix}$
34	*0*	*90*	X_1	*0*	$T_{34}=\begin{bmatrix} 1 & 0 & 0 & 0 \\ 0 & 0 & -1 & 0 \\ 0 & 1 & 0 & X_1 \\ 0 & 0 & 0 & 1 \end{bmatrix}$
45	*0*	*90*	*300*	*270*	$T_{45}=\begin{bmatrix} 0 & 0 & -1 & 0 \\ -1 & 0 & 0 & 0 \\ 0 & 1 & 0 & 300 \\ 0 & 0 & 0 & 1 \end{bmatrix}$
56	*0*	*90*	Y_1	$B+90$	$T_{56}=\begin{bmatrix} -\sin(B) & 0 & \cos(B) & 0 \\ \cos(B) & 0 & \sin(B) & 0 \\ 0 & 1 & 0 & Y_1 \\ 0 & 0 & 0 & 1 \end{bmatrix}$
6Tcp	*0*	*0*	L_{tool}	*0*	$T_{6tcp}=\begin{bmatrix} 1 & 0 & 0 & 0 \\ 0 & 1 & 0 & 0 \\ 0 & 0 & 1 & L_{tool} \\ 0 & 0 & 0 & 1 \end{bmatrix}$

At the view of Table 1 in which the element matrices are described, the final postmultiplication following the method in Eq. 6, is the resulting one shown in Eq. 11:

$$ {}^{1}_{tcp}\mathbf{T}_{th\_Channel1} = \mathbf{T}_{12}\cdot\mathbf{T}_{23}\cdot\mathbf{T}_{34}\cdot\mathbf{T}_{45}\cdot\mathbf{T}_{56}\cdot\mathbf{T}_{6tcp} = $$

$$ = \left[\begin{array}{ccc|c} -\cos(C_1)\sin(B) & \sin(C_1) & \cos(B)\cos(C_1) & -1400\cos(C_1)-X_1\cos(C_1)+L_h\cos(B)\cos(C_1)-700\sin(C_1)+Y_1\sin(C_1) \\ -\sin(B)\sin(C_1) & -\cos(C_1) & \cos(B)\sin(C_1) & 700\cos(C_1)-Y_1\cos(C_1)-1400\sin(C_1)-X_1\sin(C_1)+L_{tool}\cos(B)\sin(C_1) \\ \cos(B) & 0 & \sin(B) & -840+Z_1+L_{tool}\sin(B) \\ \hline 0 & 0 & 0 & 1 \end{array}\right] \quad (11) $$

Until now, the analysis have only been done for what is called 'Channel 1' which is defined starting from the spindle 1 to the tool tip. This channel is used only when milling tools are machining and simultaneously the workpiece is not clamped from its opposite side. However, it is known that in these types of machines depending on the function of the part and machining strategies other channels appear and they have to be analysed too.

Channel shown in Fig. 5 could be another example of what has been mentioned before. From now on that channel

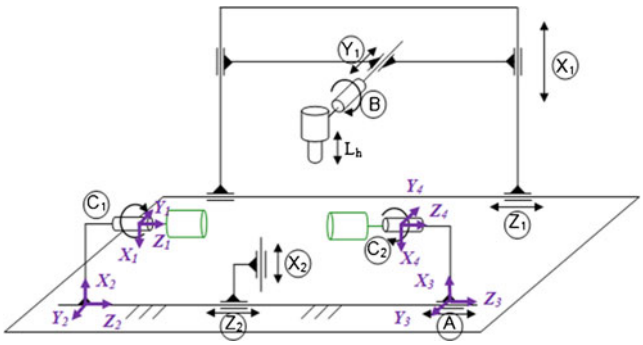

Fig. 5 General coordinate systems for the Channel 2

will be considered 'Channel 2' and the part will be clamped by the spindle 2.

As it was done for Channel 1, once the reference systems are defined for each kinematic couple following the Denavit and Hartenberg's method, the elemental transformation matrixes could be defined too. Both the parameters' values to define each matrix and the matrixes themselves are shown in Table 2.

The global transformation matrix for this channel is obtained multiplying the elemental matrixes as it has been done in Eq. 6:

$$
{}^{1}_{tcp}\mathbf{T}_{th\_Channel\,2} = \mathbf{T}_{12}\cdot\mathbf{T}_{23}\cdot\mathbf{T}_{34} =
$$

$$
= \left[\begin{array}{ccc|c}
\cos(C_1)\cos(C_2)-\sin(C_1)\sin(C_2) & -\sin(C_1)\cos(C_2)-\cos(C_1)\sin(C_2) & 0 & -1400\cos(C_1)+1400\cos(C_1)\cos(C_2)-1400\sin(C_1)\sin(C_2) \\
\sin(C_1)\cos(C_2)+\cos(C_1)\sin(C_2) & \cos(C_1)\cos(C_2)-\sin(C_1)\sin(C_2) & 0 & -1400\sin(C_1)+1400\sin(C_1)\cos(C_2)+1400\cos(C_1)\sin(C_2) \\
0 & 0 & 1 & A-2280 \\
\hline
0 & 0 & 0 & 1
\end{array}\right] \tag{12}
$$

3 Error propagation

For testing of the developed model, some error cases were analysed involving Channel 1 and Channel 2.

The importance of different type of errors is appreciated in Fig. 6, for a general machine tool and for multitasking machines. In the former, workpiece setup that must be performed between different machines and operations is the big error source. In the latter, uncertainty of alignment of the workpiece after clamping is eliminated radically, because multitasking machines always work using the same workpiece clamping and the same CNC program reference. Thus, in this kind of machine the main contribution is due to assembly errors in machine structure. On the other hand, the lack of precision between tool and collect would also be important in this distribution. That's why for checking the model those two important errors were considered, (1) positioning error and (2) imperfect tool holding (clamping) on the spindle nose error.

Once the theoretical transformation matrix was obtained for each case, the following step was to obtain the actual global matrix affected by construction errors. For this purpose, the joints between machine mobile parts were considered as non-perfect. Including the errors between the mobile elements and applying the same procedure for the definition of the theoretical matrix ($\mathbf{T_{th}}$) and the *actual global transformation matrix* ($\mathbf{T_r}$) was obtained. It depends on the errors introduced in each elemental transformation, and, as in the case of the theoretical matrix, on the dimensions of the machine and the variable axes position (value of the degrees of freedom).

As the aim of the present work is to obtain the contribution of the errors previously studied with the ideal case, a particular machine position was taken and compared in real and ideal case in Channel 1 and Channel 2. The positions were the following ones:

$C_1 = 0°$ $B = 45°$ $X_1 = 350\,\text{mm}$ $Y_1 = 175\,\text{mm}$ $Z_1 = 150\,\text{mm}$
$L_{\text{tool}} = 50\,\text{mm}$ (Channel 1) $C_1 = 0°$ $A = 1,050\,\text{mm}$ $C_2 = 0°$ (Channel 2)

The influence of the error from the analysed case on the position and the orientation of the new system respect to the theoretical case can be quantified introducing those values

Table 2 Geometrical parameters of the Denavit and Hartenberg model, Channel 2

Transaction from element i-1 to element i	a_i	α_i	d_i	θ_i	*Transformation matrix*
12	1400	0	-1140	C_1+180	$T_{12} = \left[\begin{array}{ccc\|c} -\cos(C_1) & \sin(C_1) & 0 & -1400\cos(C_1) \\ -\sin(C_1) & -\cos(C_1) & 0 & -1400\sin(C_1) \\ 0 & 0 & 1 & -1140 \\ \hline 0 & 0 & 0 & 1 \end{array}\right]$
23	0	0	A	0	$T_{23} = \left[\begin{array}{ccc\|c} 1 & 0 & 0 & 0 \\ 0 & 1 & 0 & 0 \\ 0 & 0 & 1 & A \\ \hline 0 & 0 & 0 & 1 \end{array}\right]$
34	1400	0	-1140	C_2+180	$T_{34} = \left[\begin{array}{ccc\|c} -\cos(C_2) & \sin(C_2) & 0 & -1400\cos(C_2) \\ -\sin(C_2) & -\cos(C_2) & 0 & -1400\sin(C_2) \\ 0 & 0 & 1 & -1140 \\ \hline 0 & 0 & 0 & 1 \end{array}\right]$

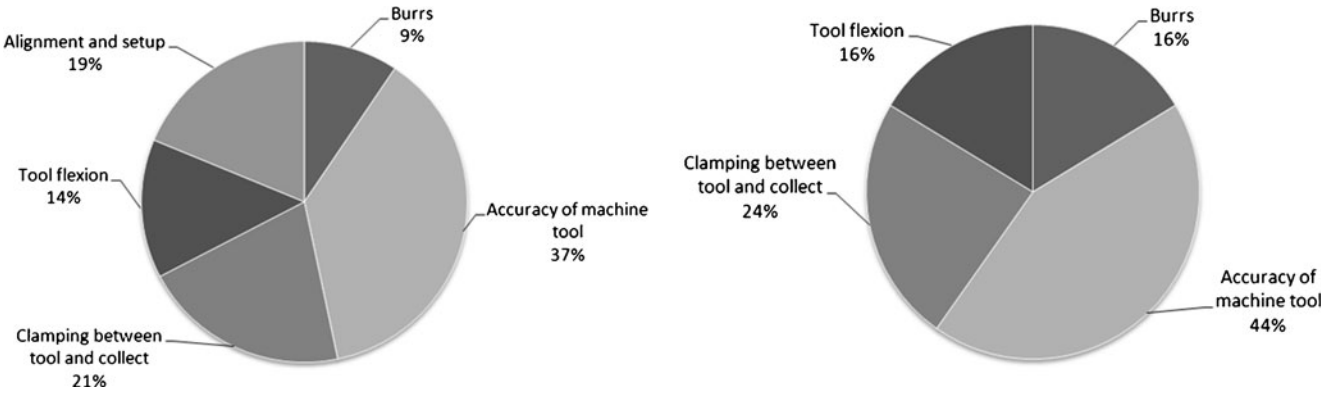

Fig. 6 Distribution of most common errors. *Left*, machine tools. *Right*, multitasking machines [28]

in the real and theoretical matrixes. The first one is easily obtained subtracting the vectors related to the Channel 1 system from the T_{th} matrix and the matrix with error T_r.

Nevertheless, to calculate the error in the orientation regarding to the ideal case, attention has to be paid to the rotation matrix $\boldsymbol{R}$. For that purpose, it has to be taken into account that the columns of the matrix are the new reference system's (*tcp* system) director cosines, which coincide with the components of the unitary vectors i_{tcp}, j_{tcp} and k_{tcp} from the original reference system (X_1, Y_1 and Z_1) expressed by $\{u\}$, $\{v\}$ and $\{w\}$.

The angles between the axes of the theoretical position and the axes after introducing an error can be obtained simply applying the definition of the vector scalar multiplication (Eq. 13) and in that way observe the deviation produced from that error.

Usually, only the error regarding to Z_{tcp} is studied because it is the axis related to milling tool axis.

$$\mathbf{w}_{th} \cdot \mathbf{w}_r = |\mathbf{w}_{th}| \cdot |\mathbf{w}_r| \cdot \cos(\varphi) \Rightarrow \cos(\varphi) = \frac{\mathbf{w}_{th} \cdot \mathbf{w}_r}{|\mathbf{w}_{th}| \cdot |\mathbf{w}_r|} \tag{13}$$

From now on, a resolution of a tenth of a micrometre for estimated errors is going to be considered for distances, even though real errors are difficult to be measured in microns (hundredth is the common resolution in a common workshop). However, this resolution is useful to compare estimated values for errors, for being able to distinguish between theoretical an error positions.

3.1 Case 1

To analyse the error in the position of the machine a particular case was chosen. Amongst all of them, a squareness error was considered, i.e. an angle between two axes was not 90° (see Fig. 7). For example, the *X*-axis of the machine would not be necessarily perpendicular to the *YZ* plane, and therefore an angular error (with two components) was introduced. In order to check the matrix formulation, an error of value 0.001° (3.6 arcsec) was taken.

In comparison with the ideal case, in Table 1 only α_i geometrical parameter was changed between the elements 2 and 3.

The theoretical matrix after including this error is shown in Appendix A.

– Matrix without error—it was obtained simply substituting the position chosen into the general matrix (Eq. 11).

$${}^{1}_{tcp}\mathbf{T}_{th\_Channel\ 1} = \left[\begin{array}{cccc} -0.70711 & 0 & 0.70711 & -1714.6447 \\ 0 & -1 & 0 & 525 \\ 0.70711 & 0 & 0.70711 & -654.6447 \\ \hline 0 & 0 & 0 & 1 \end{array}\right] \tag{14}$$

– Matrix with squareness error:

$${}^{1}_{tcp}\mathbf{T}_{r\_squareness} = \left[\begin{array}{cccc} -0.70710 & 0 & 0.70712 & -1714.6410 \\ 0 & -1 & 0 & 525 \\ 0.70712 & 0 & 0.70710 & -654.6412 \\ \hline 0 & 0 & 0 & 1 \end{array}\right] \tag{15}$$

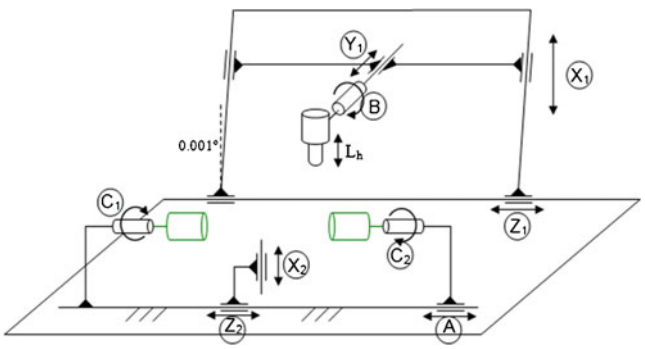

Fig. 7 Introduction of a squareness error in Channel 1

Therefore the difference position vector resulted as:

$$\Delta \mathbf{d}^{T}_{squareness} = [-0.0037 \quad 0 \quad -0.0035] \tag{16}$$

The error obtained between the theoretical and real position for this case 1 was:

$$\Delta\delta_{squareness} = \sqrt{\delta_x^2 + \delta_y^2 + \delta_z^2} = 0.0051\,mm \tag{17}$$

3.2 Case 2

Another case was to consider an assembly error between the tool holder and tool due to the collet eccentricity, in this case an angular deviation, as shown in Fig. 8. The matrix changed introducing an angular deviation of 0.001° in the tool clamping interface. Matrix is shown in Appendix B. Now, in Table 1, the geometrical parameter to change was α_i in the transaction from elements 5 to element 6.

Error between the tool and the collect:

$${}^{1}_{tcp}\mathbf{T}_{r\_clamping} = \left[\begin{array}{cccc} -0.70711 & 9.66842\cdot10^{-6} & 0.70711 & -1714.6447 \\ 0 & -1 & 1.36732\cdot10^{-5} & 525.0007 \\ 0.70711 & 9.66842\cdot10^{-6} & 0.70711 & -654.6447 \\ \hline 0 & 0 & 0 & 1 \end{array}\right] \tag{18}$$

If this case was compared with the ideal one using a difference position vector.

$$\Delta \mathbf{d}^{T}_{clamping} = [0 \quad -0.0007 \quad 0] \tag{19}$$

The error in position obtained was:

$$\Delta\delta_{clamping} = \sqrt{\delta_x^2 + \delta_y^2 + \delta_z^2} = 0.0007\,mm \tag{20}$$

This value is very low to be cause for concern.

3.3 Case 3

In the last case both previous cases of errors were taken into account simultaneously, as it is shown in Fig. 9. The matrix is shown in Appendix C.

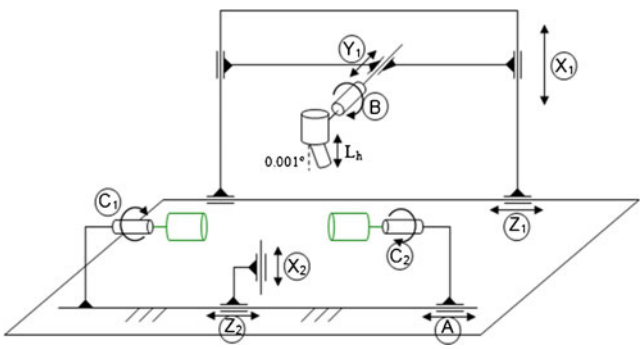

Fig. 8 Introduction of a tool clamping error in Channel 1

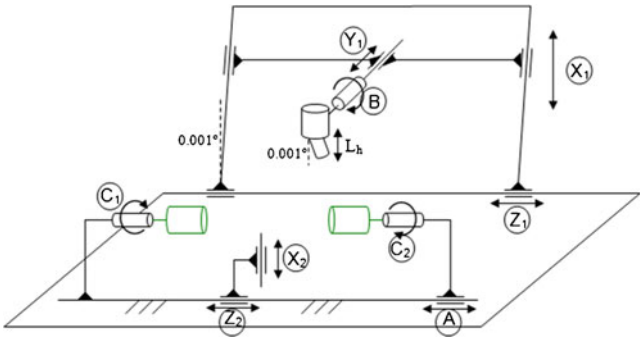

Fig. 9 Two simultaneous errors in Channel 1

Where the actual transformation matrix and the difference position vector were:

$${}^{1}_{tcp}\mathbf{T}_{r\_squa\_clam} = \left[\begin{array}{cccc} -0.70710 & 9.66852\cdot10^{-6} & 0.70712 & -1714.6410 \\ 0 & -1 & 1.36732\cdot10^{-5} & 525.0007 \\ 0.70712 & 9.66831\cdot10^{-6} & 0.70710 & -654.6412 \\ \hline 0 & 0 & 0 & 1 \end{array}\right] \tag{21}$$

$$\Delta \mathbf{d}^{T}_{squa\_clam} = [-0.0037 \quad -0.0007 \quad -0.0035] \tag{22}$$

And the error was:

$$\Delta\delta_{squa\_clam} = \sqrt{\delta_x^2 + \delta_y^2 + \delta_z^2} = 0.0051\ mm \tag{23}$$

At the view of these outcomes, the final result is a linear combination of previous ones. The resultant models provide the real position of the tool as a function of the position of the degrees of freedom. Position is given by the tool tip Cartesian coordinates and the tool orientation is provided by the tool axis (axis Z_{tcp}). So, it can be obtained the real path followed by the tool tip and its orientation for a set of different positions of the degrees of freedom, being compared with the theoretical ones. In this way, the error map for the complete spatial machine movements in the whole work volume of the five-axis machine can be obtained, as it is made in Refs. [16, 22].

Each elemental matrix includes the geometrical simple errors. Then, the *actual global transformation matrix* is obtained by the multiplication of the elemental matrices. For the above example, the final real matrix $\mathbf{T}_r$ results in:

$${}^{1}_{tcp}\mathbf{T}_{r\_Channel\,1} = \mathbf{T}_{12}\cdot\mathbf{T}_{23}\cdot\mathbf{T}_{34\_error}\cdot\mathbf{T}_{45}\cdot\mathbf{T}_{56\_error}\cdot\mathbf{T}_{6tcp} \tag{24}$$

After the error estimation at the tool tip, one possibility is trying to compensate it changing the machine position to achieve an exact spatial position, as it is explained in [22] solving the inverse kinematics problem. Other possibility is to include the *real transformation matrix* for a particular milling machine in the internal CNC kinematics model to be used by the interpolation functions. In this way, an improved

accuracy would be achieved without machine user intervention.

3.4 Case 4

Although it has been mentioned in Fig. 6 that multitasking machines do not present errors related to the alignment of the part, as the operations are done in the same part clamping, in this case a misalignment between the two main spindles was considered (see Fig. 10). This machine type can change part between left chuck and right chunk, so this error could affect part precision.

This case has a particular interest because it is known that a particular company, because of a collision during machining, had both spindles damaged causing a severe misalignment with an estimated maximum value of 0.003° out of squareness. As a consequence, spindle 1 held the part perfectly, while the part in spindle 2 had a certain inclination due to the misalignment induced by the previous collision.

The matrix obtained using Denavit and Hartenberg is shown in Appendix D.

The theoretical matrix obtained after introducing the machine's position in Eq. 12 was the following:

$$ {}^{1}_{4}\mathbf{T}_{th\_Channel\ 2} = \left[\begin{array}{ccc|c} 1 & 0 & 0 & 0 \\ 0 & 1 & 0 & 0 \\ 0 & 0 & 1 & -1230 \\ \hline 0 & 0 & 0 & 1 \end{array}\right] \tag{25} $$

Once the error was introduced, from the postmultiplication of the elementary matrixes the global transformation matrix $\boldsymbol{T_r}$ was obtained:

$$ {}^{1}_{4}\mathbf{T}_{r\_Channel\ 2} = \mathbf{T}_{12} \cdot \mathbf{T}_{23\_error} \cdot \mathbf{T}_{34} \tag{26} $$

$$ {}^{1}_{4}\mathbf{T}_{r\_misalignment} = \left[\begin{array}{ccc|c} 1 & 5.24\cdot10^{-5} & 0 & 0 \\ 5.24\cdot10^{-5} & 1 & 0 & -0.07336 \\ 0 & 0 & 1 & -1230 \\ \hline 0 & 0 & 0 & 1 \end{array}\right] \tag{27} $$

From the difference between the two vectors the error vector of position could be obtained:

$$ \Delta\mathbf{d}^{T}_{misalignment} = [\,0 \quad 0.07336 \quad 0\,] \tag{28} $$

And the error:

$$ \Delta\delta_{misalignment} = \sqrt{\delta_x^2 + \delta_y^2 + \delta_z^2} = 0.07336\ mm \tag{29} $$

This value is in the order of hundredths of millimetre, and to be considered for reduction.

3.5 Case 5

As what appears in Fig. 11, now, the three cases of error analysed before were introduced simultaneously: squareness, clamping and misalignment errors. This case would be only considered if the workpiece was transferred from left headstock (spindle 1) to the right one (spindle 2) for being machined in both ends, which is not the general case.

Using results from cases 3 and 4, theoretical and real positions of the tool centre point with respect to the original coordinate system $X_1\ Y_1\ Z_1$ and of the spindle 2 with respect to the same system were:

$$ {}^{1}_{tcp}\mathbf{d}^{T}_{th} = [\,-1,714.6447 \quad 525 \quad -654.6447\,] \tag{30} $$

$$ {}^{1}_{tcp}\mathbf{d}^{T}_{r} = [\,-1,714.6410 \quad 525.0007 \quad -654.6412\,] \tag{31} $$

$$ {}^{1}_{4}\mathbf{d}^{T}_{\mathrm{th}} = [\,0 \quad 0 \quad -1,230\,] \tag{32} $$

$$ {}^{1}_{4}\mathbf{d}^{T}_{r} = [\,0 \quad -0.07336 \quad -1,230\,] \tag{33} $$

Applying the above equations, theoretical and real distance vector between tool centre point and spindle 2

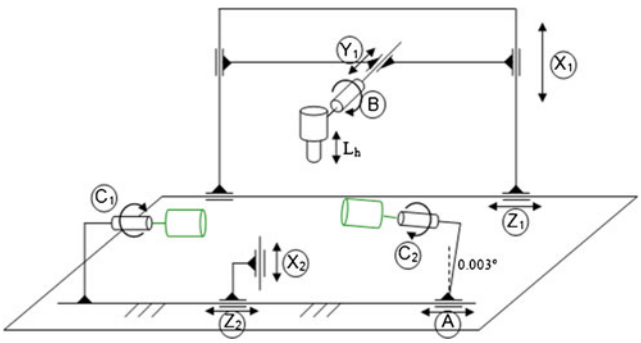

Fig. 10 Introduction of a misalignment error in Channel 2

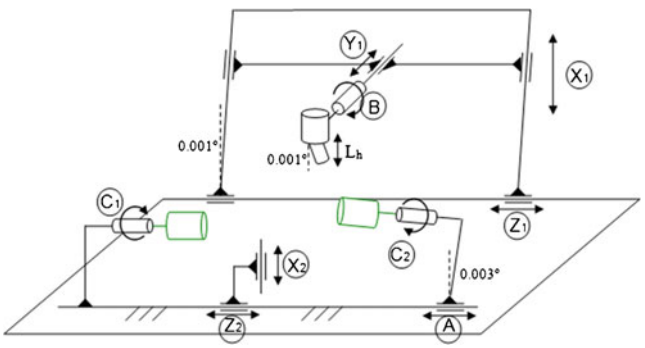

Fig. 11 Introduction of all previous cases of errors simultaneously

(considering a workpiece clamped into it with a null length) were:

$$ {}^{4}_{tcp}\mathbf{d}^{T}_{th} = [\,-1,714.6447 \quad 525 \quad 575.3553\,] \tag{34} $$

$$ {}^{4}_{tcp}\mathbf{d}^{T}_{r} = [\,-1,714.6410 \quad 525.0741 \quad 575.3588\,] \tag{35} $$

Being the difference between them the error vector:

$$ {}^{4}_{tcp}\Delta\mathbf{d}^{T}_{squa\_clamp\_misa} = [\,-0.0004 \quad -0.0741 \quad -0.0004\,] \tag{36} $$

So the value of the error in this case was,

$$ \Delta\delta_{squa\_clamp\_misa} = \sqrt{\delta_x^2 + \delta_y^2 + \delta_z^2} = 0.0741\ mm \tag{37} $$

4 Results of some errors for different machine positions

Firstly, the work was done in Channel 1. Like was done beforehand, by Denavit and Hartenberg method some errors at the tool tip (δ_X, δ_Y and δ_Z) were estimated for two simultaneous errors and three different values of them in. The values of the degree of freedom, as same as in case 3, were the next ones:

$C_1 = 0^\circ \quad B = 45^\circ \quad X_1 = 350\ mm \quad Y_1 = 175 \quad mm$
$Z_1 = 150mm \quad L_{tool} = 50\ mm$

The solutions are recorded in Table 3.

Table 3 Example of some errors

Squareness error	Fixation error	δ_x (mm)	δ_y (mm)	δ_z (mm)	$\Delta\delta$ (mm)
0.001°	0.001°	−0.0037	−0.0007	−0.0035	0.001
0.002°	0.001°	−0.0104	−0.0007	−0.0098	0.0144
0.004°	0.001°	−0.0238	−0.0007	−0.0224	0.0327
0.001°	0.002°	−0.0037	−0.0017	−0.0035	0.0053
0.002°	0.002°	−0.0104	−0.0017	−0.0098	0.0144
0.004°	0.002°	−0.0124	−0.0017	−0.0116	0.0171

At the view of the results a rapid conclusion is extracted: when the squareness error gets higher both the total error and its components x and z get higher while y maintains its value. The last one only changes when the fixation error changes. It is clear that the influence of increasing the value of clamping error is not appreciated directly in the total error.

Continuing with the study, it was analysed what influence each degree of freedom had in the tool tip position. For that purpose, different machine positions were chosen and case 3 was solved. In each one, only 1 degree of freedom was changed: the translational degrees of freedom are reduced in 30 % and the rotational ones at −45°. Position number one corresponds to the initial position previously analysed in Sections 3.1, 3.2 and 3.3.

Position No. 1 : $C_1 = 0^\circ \quad B = 45^\circ \quad X_1 = 350\,\text{mm} \quad Y_1 = 175\,\text{mm} \quad Z_1 = 150\,\text{mm} \quad L_{\text{tool}} = 50\,\text{mm}$
Position No. 2 : $\mathbf{C_1 = -45^\circ} \quad B = 45^\circ \quad X_1 = 350\,\text{mm} \quad Y_1 = 175\,\text{mm} \quad Z_1 = 150\,\text{mm} \quad L_{\text{tool}} = 50\,\text{mm}$
Position No. 3 : $C_1 = 0^\circ \quad \boldsymbol{B = 0^\circ} \quad X_1 = 350\,\text{mm} \quad Y_1 = 175\,\text{mm} \quad Z_1 = 150\,\text{mm} \quad L_{\text{tool}} = 50\,\text{mm}$
Position No. 4 : $C_1 = 0^\circ \quad B = 45^\circ \quad \boldsymbol{X_1 = 245\,mm} \quad Y_1 = 175\,\text{mm} \quad Z_1 = 150\,\text{mm} \quad L_{\text{tool}} = 50\,\text{mm}$
Position No. 5 : $C_1 = 0^\circ \quad B = 45^\circ \quad X_1 = 350\,\text{mm} \quad \boldsymbol{Y_1 = 123\,mm} \quad Z_1 = 150\,\text{mm} \quad L_{\text{tool}} = 50\,\text{mm}$
Position No. 6 : $C_1 = 0^\circ \quad B = 45^\circ \quad X_1 = 350\,\text{mm} \quad Y_1 = 175\,\text{mm} \quad \boldsymbol{Z_1 = 105\,mm} \quad L_{\text{tool}} = 50\,\text{mm}$

Obtaining the Denavit and Hartenbeng actual transformation matrix $\mathbf{T_{r3}}$ (Eq. 14) for each position, and comparing with the theoretical matrix $\mathbf{T_{th\_Channel\ 1}}$ before substituting the new position, the errors shown in Table 4 appeared.

Analysing the effect of the translational and rotational degrees of freedom separately, it can be observed how the positions No. 1, 2, 5, and 6 are the ones which contribute more to the error. These positions coincide with the variation of the rotation C_1 and B and the translation of Y_1 and Z_1 respectively, being those the degrees of freedom with most influence in the error propagation.

Having known which degrees of freedom are the most influential it could be interesting to study its variation throughout the trajectory. Main characteristics of the studied model were based on a medium size machine typical for automotive components manufacturing. The stroke of Y_1-

Table 4 Value of error for different positions of machine

Machine position	δ_x (mm)	δ_y (mm)	δ_z (mm)	$\Delta\delta$ (mm)
No. 1	−0.0037	−0.0007	−0.0035	*0.0051*
No. 2	−0.0031	0.0021	−0.0035	*0.0051*
No. 3	−0.0033	−0.0007	−0.0033	0.0047
No. 4	−0.0037	−0.0007	−0.0023	0.0044
No. 5	−0.0037	−0.0007	−0.0035	*0.0051*
No. 6	−0.0037	−0.0007	−0.0035	*0.0051*

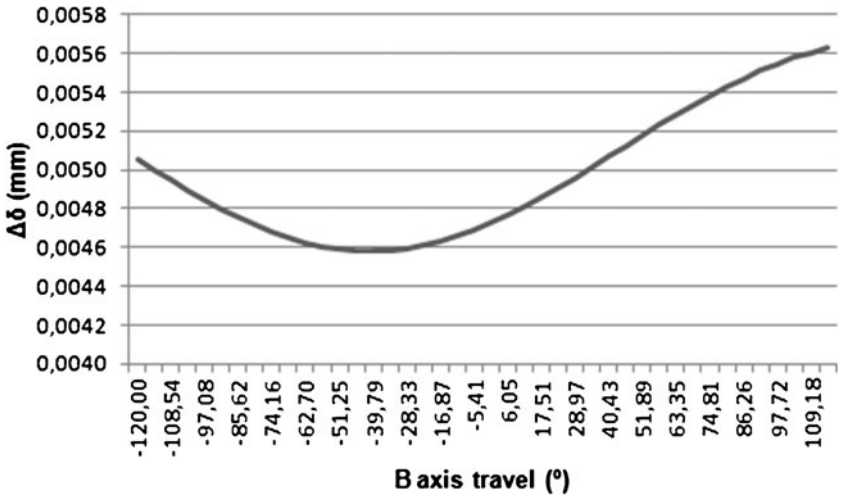

Fig. 12 Error variation along *B*-axis rotation

axis and Z_1-axis is ±210 mm for the first one and 1,120 mm for the second one; in rotational axes, the trajectory is ±120° for *B*-axis and 0º−360º for C_1-axis.

Once all the previous cases have been analysed, an error higher than a micron has only been appreciated in the rotational *B*-axis as it can be seen in Fig. 12.

As it can be seen in the graph, positioning error decreases when B-axis is between −120° and 0°, reaching a minimum value of 0.0046 mm. However, when the axis works in positive angles the error arises to 0.0056 mm. With this, it can be concluded that the positioning error can reach ±0.00100÷360°mm in comparison to the ideal case.

As well as in Channel 1, in Channel 2 the influence of the degrees of freedom C_1, C_2 and *A* have been analysed regarding to the misalignment error. In this case, the variation of the degrees of freedom has no significant error.

5 Consequences of errors on continuous machining

In order to visually distinguish how these errors affect the final pieces and their consequences on them, the full simulation of a machining process was carried out. In this way, the systematic effect of error in final parts can be considered. The example case shown below, is related to the manufacturing of a tool holder under standard ISO 26623-1: 2008 'Polygonal taper interface with flange contact surface—part 1: dimensions and designation of shanks', whose tapered shape errors could be dramatically affected by cases 1 and 2 errors (see Sections 3.1 and 3.2). As this piece is always performed with raw part clamped on the spindle 1, there is no effect of error in Channel 2. Channel 2 error would only appear if machined part is re-clamped into the right spindle for further operations, not the case here.

The virtual verification module of the CAM software ESPRIT® to generate CAM operations was chosen. Only for magnification purposes it was necessary to introduce a higher error for cases 1 and 2, considering 6° instead of 0.001°, to have a better appreciation of the error. Although this consideration was too higher to be a real case, it helps to show the difference between real and theoretical parts.

The operation studied was performed by the main spindle (swivelling the *B*-axis at the end of the octagonal ram). This operation is very important because the tool holder trigonal surface is defined in the ISO standard to accomplish.

Figure 13 compares the differences between real and theoretical cases, once the errors mentioned in Sections 3.1 and 3.2 of squareness and clamping were introduced. Hence, row 1 shows the effect of squareness error in the reference position of the machine tool, just previous to run the CNC program. Row 2 shows for the same position the introduction of the tool holder clamping error, introducing the equivalent angular error on headstock. In the last row, how the milling operation is clearly affected by both simultaneous errors is reflected; as shown on the right hand column, there is distortion of the trigonal surface.

Once the machining process was simulated, it was time to compare volumes of perfect and wrongly machined trigonal surface. As Fig. 14 shows, the introduction of squareness and clamping errors result in a part out of tolerance required by the standard. The blue one (dark-coloured volume) is the theoretical part whereas the yellow one (light-coloured volume) is the part obtained considering there is 6° of squareness and

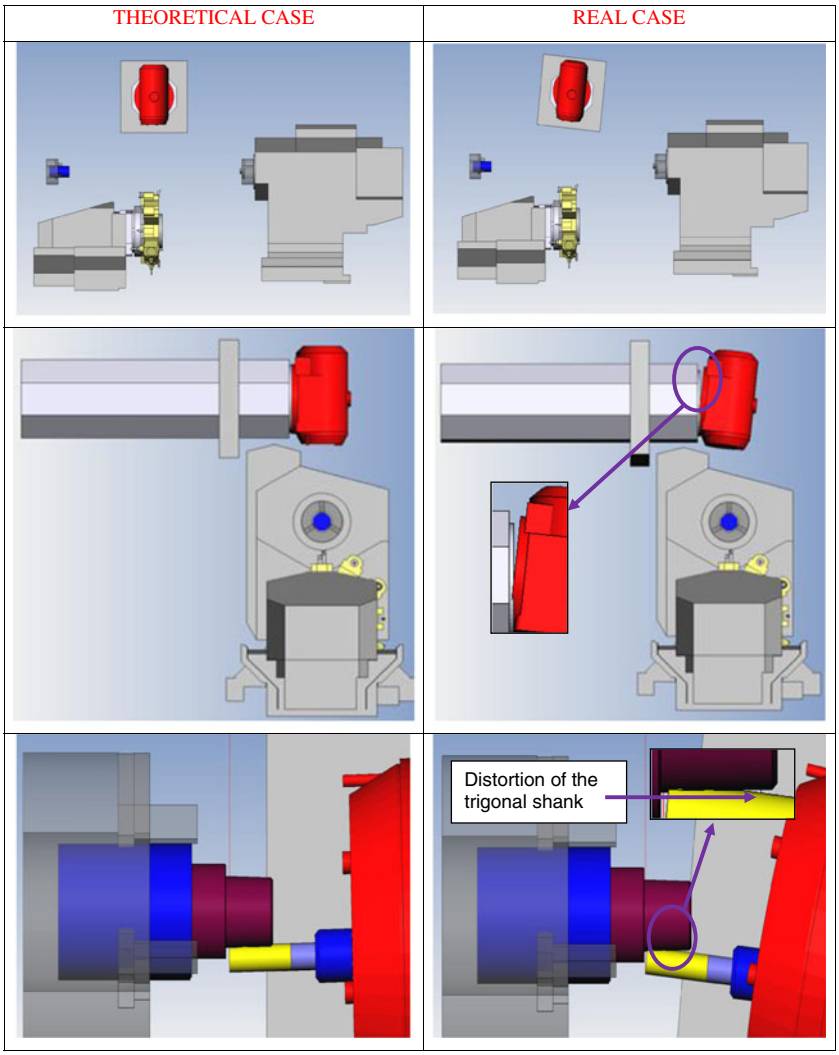

Fig. 13 Simulation of the process

clamping error. Figure 14 shows values of maximum deviations for real expected errors but also for exaggerated values, the latter for a most visual representation of consecuences.

For this application, the maximum error of 3 μm could be accepted since after milling a grinding process of the trigonal surface is always performed; the error is eliminated by grinding absolutely.

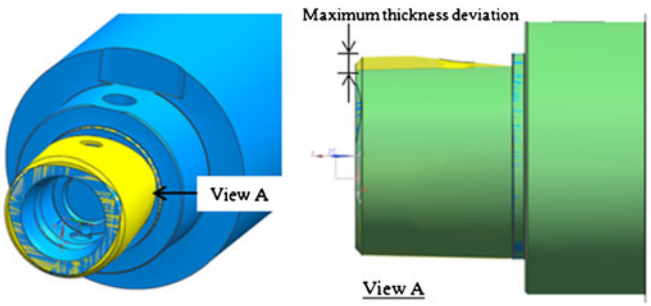

Error introduced	Maximum thickness deviation
Squareness: 0.001° Clamping: 0.001°	3 μm
Squareness: 1° Clamping: 1°	32 μm
Squareness: 6° Clamping: 6°	158 μm

Fig. 14 CAD volumes comparison and error values (scaled for a better view). *Left*, isometric and lateral view of the trigonal-shaped shank (error introduced, 6°). *Right*, values of maximum thickness deviation due to three cases of error introduced

6 Conclusions

In this work, a useful methodology to estimate global precision of complex multitasking machines is presented, based on the use of Denavit and Hartenberg's formulation. In this kind of machine, an elemental error in one joint affects both the position and orientation of the tool, causing that final part to be out of tolerances and with form deviation.

Elemental errors have been defined for a multitasking machine. The way to introduce them in the **T** matrices has been fully described. With the theoretical matrix formulation, the real effect of each of the assembly errors is estimated. Therefore, those with more weight on tool tip error would be the first objective to be reduced at the assembly stage of the machine tool.

In assembled machines placed in workshops, the use of the proposed methodology can be useful to define machine positions where some errors are the minimums. Machine tools manufacturers can in this way help their customers to improve the accuracy of the final parts produced.

Acknowledgements Thanks are addressed to "EUSPEN challenge of Spain" for the opportunity to work about this research line. Thanks are given to Sabino Azkarate from Tekniker for the valuable suggestions in the organisation of Euspen competition.

Appendix A. Transformation matrix of the squareness error

$$ {}^{1}_{tcp}\mathbf{T}_{r\_squareness} = \begin{bmatrix} {}^{1}_{tcp}\mathbf{R} & {}^{1}_{tcp}\mathbf{d} \\ \mathbf{0} & 1 \end{bmatrix} $$

$$ {}^{1}_{tcp}\mathbf{R} = \begin{bmatrix} 1.10196\cdot 10^{-5}\cos(B)\cos(C_1) - \cos(C_1)\sin(B) & \sin(C_1) & \cos(B)\cos(C_1) + 1.10196\cdot 10^{-5}\cos(C_1)\sin(B) \\ 1.10196\cdot 10^{-5}\cos(B)\sin(C_1) - \sin(B)\sin(C_1) & -\cos(C_1) & 1.10196\cdot 10^{-5}\sin(B)\sin(C_1) + \cos(B)\sin(C_1) \\ \cos(B) + 1.10196\cdot 10^{-5}\sin(B) & 0 & -1.10196\cdot 10^{-5}\cos(B) + \sin(B) \end{bmatrix} $$

$$ {}^{1}_{tcp}\mathbf{d} = \begin{bmatrix} -X_1\cos(C_1) + 1.10196\cdot 10^{-5}\cdot 300\cos(C_1) - 1,400\cos(C_1) + L_{\text{tool}}[\cos(B)\cos(C_1) + 1.10196\cdot 10^{-5}\cos(C_1)\sin(B)] - 700\sin(C_1) + Y_1\sin(C_1) \\ 700\cos(C_1) - Y_1\cos(C_1) + L_{\text{tool}}[1.10196\cdot 10^{-5}\sin(B)\sin(C_1) + \cos(B)\sin(C_1)] - X_1\sin(C_1) + 1.10196\cdot 10^{-5}\cdot 300\sin(C_1) - 1,400\sin(C_1) \\ -840 + 1.10196\cdot 10^{-5}X_1 + Z_1 + L_{\text{tool}}[-1.10196\cdot 10^{-5}\cos(B) + \sin(B)] \end{bmatrix} $$

Appendix B. Transformation matrix of the tool clamping error

$$ {}^{1}_{tcp}\mathbf{T}_{r\_clamping} = \begin{bmatrix} {}^{1}_{tcp}\mathbf{R} & {}^{1}_{tcp}\mathbf{d} \\ \mathbf{0} & 1 \end{bmatrix} $$

$$ {}^{1}_{tcp}\mathbf{R} = \begin{bmatrix} -\cos(C_1)\sin(B) & 1.36732\cdot 10^{-5}\cos(B)\cos(C_1) + \sin(C_1) & \cos(B)\cos(C_1) - 1.36732\cdot 10^{-5}\sin(C_1) \\ -\sin(B)\sin(C_1) & -\cos(C_1) + 1.36732\cdot 10^{-5}\cos(B)\sin(C_1) & 1.36732\cdot 10^{-5}\cos(C_1) + \cos(B)\sin(C_1) \\ \cos(B) & 1.36732\cdot 10^{-5}\sin(B) & \sin(B) \end{bmatrix} $$

$$ {}^{1}_{tcp}\mathbf{d} = \begin{bmatrix} -1,400\cos(C_1) - X_1\cos(C_1) + L_{\text{tool}}[\cos(B)\cos(C_1) - 1.36732\cdot 10^{-5}\sin(C_1)] - 700\sin(C_1) + Y_1\sin(C_1) \\ 700\cos(C_1) - Y_1\cos(C_1) - 1,400\sin(C_1) - X_1\sin(C_1) + L_{\text{tool}}[\cos(B)\sin(C_1) + 1.36732\cdot 10^{-5}] \\ -840 + Z_1 + L_{\text{tool}}\sin(B) \end{bmatrix} $$

Appendix C. Transformation matrix of the combined squareness and clamping error

$$ {}^{1}_{tcp}\mathbf{T}_{r\_squa\_clam} = \begin{bmatrix} {}^{1}_{tcp}\mathbf{R} & {}^{1}_{tcp}\mathbf{d} \\ \mathbf{0} & 1 \end{bmatrix} $$

$$ {}^{1}_{tcp}\mathrm{R} = \begin{bmatrix} {}^{1}_{tcp}\mathrm{R}^{1} & {}^{1}_{tcp}\mathrm{R}^{2} & {}^{1}_{tcp}\mathrm{R}^{3} \end{bmatrix} $$

$$ {}^{1}_{tcp}\mathbf{R}^{1} = \begin{bmatrix} 1.10196 \cdot 10^{-5}\cos(B)\cos(C_1) - \cos(C_1)\sin(B) \\ 1.10196 \cdot 10^{-5}\cos(B)\sin(C_1) - \sin(B)\sin(C_1) \\ \cos(B) + 1.10196 \cdot 10^{-5}\sin(B) \\ 0 \end{bmatrix} $$

$$ {}^{1}_{tcp}\mathbf{R}^{2} = \begin{bmatrix} 1.36732 \cdot 10^{-5}\cos(B)\cos(C_1) + 1.50673 \cdot 10^{-10}\cos(C_1)\sin(B) + \sin(C_1) \\ -\cos(C_1) + 1.50673 \cdot 10^{-10}\sin(B)\sin(C_1) + 1.36732 \cdot 10^{-5}\cos(B)\sin(C_1) \\ -1.50673 \cdot 10^{-10}\cos(B) + 1.36732 \cdot 10^{-5}\sin(B) \\ 0 \end{bmatrix} $$

$$ {}^{1}_{tcp}\mathbf{R}^{3} = \begin{bmatrix} \cos(B)\cos(C_1) + 1.10196 \cdot 10^{-5}\cos(C_1)\sin(B) - 1.36732 \cdot 10^{-5}\sin(C_1) \\ 1.36732 \cdot 10^{-5}\cos(C_1) + 1.10196 \cdot 10^{-5}\sin(B)\sin(C_1) + \cos(B)\sin(C_1) \\ -1.10196 \cdot 10^{-5}\cos(B)\sin(B) \\ 0 \end{bmatrix} $$

$$ {}^{1}_{tcp}\mathbf{d}^{T} = \begin{bmatrix} -X_1\cos(C_1) + 3.30588 \cdot 10^{-3}\cos(C_1) - 1,400\cos(C_1) + L_{\text{tool}}[\cos(B)\cos(C_1) + 1.10196 \cdot 10^{-5}\cos(C_1)\sin(B) - 1.36732 \cdot 10^{-5}\sin(C_1]) - 700\sin(C_1) + Y_1\sin(C_1) \\ 700\cos(C_1) - Y_1\cos(C_1) + L_{\text{tool}}[1.36732 \cdot 10^{-5}\cos(C_1) + 1.10196 \cdot 10^{-5}\sin(B)\sin(C_1) + \cos(B)\sin(C_1)] - X_1\sin(C_1) + 3.30588 \cdot 10^{-3}\sin(C_1) - 1,400\sin(C_1) \\ -840 + 1.10196 \cdot 10^{-5}X_1 + Z_1 + L_{\text{tool}}[-1.10196 \cdot 10^{-5}\cos(B) + \sin(B)] \end{bmatrix} $$

Appendix D. Transformation matrix of misalignment between both spindles

$$ {}^{1}_{4}\mathbf{T}_{r\_desalignment} = \begin{bmatrix} {}^{1}_{4}\mathbf{R} & {}^{1}_{4}\mathbf{d} \\ \mathbf{0} & 1 \end{bmatrix} $$

$$ {}^{1}_{4}\mathbf{R} = \begin{bmatrix} \cos(C_2)[5.24 \cdot 10^{-4}\sin(C_1) + \cos(C_1)] - \sin(C_2)[-5.24 \cdot 10^{-4}\cos(C_1) + \sin(C_1)] & -\cos(C_2)[-5.24 \cdot 10^{-4}\cos(C_1) + \sin(C_1)] - \sin(C_2)[\cos(C_1) + 5.24 \cdot 10^{-4}\sin(C_1)] & 0 \\ -\cos(C_2)[5.24 \cdot 10^{-4}\cos(C_1) - \sin(C_1)] + \sin(C_2)[\cos(C_1) + 5.24 \cdot 10^{-4}\sin(C_1)] & \cos(C_2)[\cos(C_1) + 5.24 \cdot 10^{-4}\sin(C_1)] + \sin(C_2)[5.24 \cdot 10^{-4}\cos(C_1) + \sin(C_1)] & 0 \\ 0 & 0 & 1 \end{bmatrix} $$

$$ {}^{1}_{4}\mathbf{d} = \begin{bmatrix} -1,400\cos(C_1) + 1,400\cos(C_2)[\cos(C_1) + 5.24 \cdot 10^{-4}\sin(C_1)] - 1,400\sin(C_2)[-5.24 \cdot 10^{-4}\cos(C_1) + \sin(C_1)] \\ -1,400\cos(C_2)[5.24 \cdot 10^{-4}\cos(C_1) - \sin(C_1)] - 1,400\sin(C_1) + 1,400\sin(C_2)[\cos(C_1) + 5.24 \cdot 10^{-4}\sin(C_1)] \\ A - 2,280 \end{bmatrix} $$

References

1. Lamikiz A, López de Lacalle LN (2009) Machine tools: a general view, machine tools for high performance machining. Springer, Berlin
2. Rahman M (2004) Modelling and measurement of multi-axis machine tools to improve positioning accuracy in a software way. Ph.D. thesis, University of Oulu, Finland
3. Ramesh R, Mannan MA, Poo AN (2000) Error compensation in machine tools—a review: part I: geometric, cutting-force induced and fixture-dependent errors. Int J Mach Tool Manuf 40(9):1235–1256
4. Slocum A (1992) Precision machine design. Prentice-Hall, Englewood Cliffs
5. Masaomi Tsutsumi S, Saito A (2004) Identification of angular and positional deviations inherent to 5-axis machining centres with a tilting-rotary table by simultaneous four-axis control movements. Int J Mach Tool Manuf 44:1333–1342
6. Srivasta A, Veldhuis MA (1995) Modelling geometric and thermal errors in five-axes CNC machine tool. Int J Mach Tool Manuf 35:1321–1337

7. Nawara L, Kowalski J, Sladek J (1989) The influence of kinematic errors on the profile shapes by means of CMM. Ann CIRP 38 (1):511–516
8. Soons J, Theuws F, Schllekens P (1992) Modelling the errors of multi axis machines: a general methodology. Precis Eng 14(1):5–19
9. Suh SH, Lee JJ, Kim SK (1998) Multiaxis machining with additional-axis NC system: theory and development. Int J Adv Manuf Technol 14:865–875
10. Ferreira P, Liu C (1989) An analytical quadratic model for the geometric errors of a machine tool. J Manuf Syst 5(1):51–63
11. Mou J, Liu CR (1995) A method for enhancing the accuracy of CNC machine tools for on-machine inspection. J Manuf Syst 11 (4):29–237
12. Sørby K (2007) Inverse kinematics of five-axis machines near singular configurations. Int J Mach Tool Manuf 47(2):299–306
13. Cho J, Cho M, Kim K (1994) Volumetric error analysis of a multi-axis machine tool machining a sculptured workpiece. Int J Prod Res 32(2):345–363
14. Jha BK, Kumar A (2003) Analysis of geometric errors associated with five-axis machining centre in improving the quality of cam profile. Int J Mach Tool Manuf 43:629–636
15. Lei WT, Hsu YY (2002) Accuracy test of five-axis CNC machine tool with 3D probe-ball. Part II: errors estimation. Int J Mach Tool Manuf 42:1163–1170
16. Lin PD, Ehmann KF (1993) Direct volumetric error evaluation for multi-axis machines. Int J Mach Tool Manuf 33(5):675–693
17. Lee RS, She CH (1997) Developing a postprocessor for three types of five-axis machine tools. Int J Adv Manuf Technol 13(9):658–665
18. Lin YJ, Shen YJ (2003) Modelling of five-axis machine tool metrology models using the matrix summation approach. Int J Adv Manuf Technol 21(4):243–248
19. Mahbubur RMD, Heikkala J, Lappalainen K, Karjalainen JA (1997) Positioning accuracy improvement in five-axis milling by post processing. Int J Mach Tool Manuf 37(2):223–236
20. Remus T-FO, Feng H-Y (2004) Configuration analysis of five-axis machine tools using a generic kinematic model. Int J Mach Tool Manuf 44(11):1235–1243
21. Moon SK, Moon Y-M, Kota S (2001) Screw theory based metrology for design and error compensation of machine tools. Proceedings of DETC'01: ASME 2001 Design Engineering Technical Conferences, Pittsburgh, Pennsylvania, 9–12 September
22. Lee E, Suh S, Shon J (1998) A comprehensive method for calibration of volumetric positioning accuracy of CNC-machines. Int J Adv Manuf Technol 14:43–49
23. Raksiri C, Parnichkun M (2004) Geometric and force errors compensation in a 3-axis CNC milling machine. Int J Mach Tool Manuf 44(12–13):1283–1291
24. Chen G, Yuan J, Ni J (2001) A displacement measurement approach for machine geometric error assessment. Int J Mach Tool Manuf 41(1):149–161
25. Sartori S, Zhang GX (1995) Geometric error measurement and compensation of machines. Ann CIRP 44(2):99–609
26. Fan K, Lin J, Lu S, (1996) Measurement and compensation of thermal error on a machining centre. In: Proceedings of the fourth International conference on automatic technology, Hsinchu, Taiwan, 8–11 July 1996, pp. 261–268
27. Salgado MA, López de Lacalle LN, Lamikiz A, Muñoa J, Sánchez JA (2005) Evaluation of the stiffness chain on the deflection of end-mills under cutting forces. Int J Mach Tool Manuf 45:727–739
28. Uriarte L, Herrero A, Zatarain M, Santiso G, Lopéz de Lacalle LN, Lamikiz A, Albizuri J (2007) Error budget and stiffness chain assessment in a micromilling machine equipped with tools less than 0.3 mm in diameter. Precis Eng 31(n.1):1–12
29. Armarego EJA, Deshpande NP (1991) Computerized end-milling force predictions with cutting models allowing for eccentricity and cutter deflections. Ann CIRP 40(1):25–29
30. López de Lacalle LN, Lamikiz A, Sánchez JA, Salgado MA (2004) Effects of tool deflection in the high speed milling of inclined surfaces. Int J Adv Manuf Technol 24(9):621–631
31. Kim GM, Kim BH, Chu CN (2003) Estimation of cutter deflection and form error in ball-end milling process. Int J Mach Tool Manuf 43:917–924
32. López de Lacalle LN, Lamikiz A, Sánchez JA, Salgado MA (2007) Toolpath selection based on the minimum deflection cutting forces in the programming of complex surfaces milling. Int J Mach Tool Manuf 47(2):388–400
33. Ikua BW, Tanaka H, Obata F, Sakamoto S (2001) Prediction of cutting forces and machining error in ball end milling of curved surfaces-I theoretical analysis. Precis Eng 25:266–273
34. Donaldson RR (1980) Error budgets. In: Hocken RJ (ed) Technology of machine tool. Machine tool accuracy, vol.5, Ch 9. Machine Tool Task Force
35. Walter MM, Norlund B, Koning RJ, Roblee JW (2002) Error budget as a design tool for ultra-precision diamond turning machines. In: ASPE's 17th Annual Meeting, 20–25 October 2002
36. Treib T, Matthias E (1987) Error budgeting—applied to the calculation and optimization of the volumetric error field of multiaxis systems. Ann CIRP 36(1):365–368
37. Lee JH, Liu Y, Yang SH (2006) Accuracy improvement of miniaturized machine tool: geometric error modeling and compensation. Int J Mach Tool Manuf 46(12–13):1508–1516
38. Huertas Talón JL, Boria DR, Muro LB, Gómez CL, Zurdo JJM, Calvo FV, Barace JJG (2011) Functional check test for high-speed milling centres of up to five axes. Int J Adv Manuf Technol 55(1–4):39–52
39. Zargarbashi SHH, Mayer JRR (2006) Assessment of machine tool trunnion axis motion error, using magnetic double ball bar. Int J Mach Tool Manuf 46(14):1823–1834
40. Lee KI, Lee DM, Kweon SH, Yang SH (2010) Geometric errors estimation of a rotary table using double ball-bar. J Korean Soc Precis Eng 27(11):98–105
41. López de Lacalle LN, Lamikiz A, Sanchez JA, Ocerin O, Maidagan E (2008) The Denavit and Hartenberg approach applied to evaluate the consequences in the tool tip position of geometrical errors in five-axis milling centres. International Journal of Advanced Manufacturing Technology 37(1–2):122–139
42. ISO 230-1:1996: Test code for machine tools—part 1: geometric accuracy of machines operating under no-load or quasi-static conditions
43. ISO 10791-2:2001: Test conditions for machining centres—part 2: geometric tests for machines with vertical spindle or universal heads with vertical primary rotary axis (vertical *Z*-axis)
44. ISO 10791-1:1998: Test conditions for machining centres—part 1: geometric tests for machines with horizontal spindle and with accessory heads (horizontal *Z*-axis)
45. Rocha CR, Tonetto CP, Dias A (2011) A comparison between the Denavit–Hartenberg and the screw-based method used in kinematic modeling of robot manipulators. Robot Comput Integr Manuf 27:723–728